Adsorption of Heavy Metals from Aqueous Solution onto Sawdust Activated Carbon

Marah W. Khalid*   **Sami D. Salman****

*,**Department of Biochemical Engineering/ Al-khwarizmi College of Engineering/ University of Baghdad/ Iraq*
*Email: sami.albayati@gmail.com

Abstract

In this study, sawdust as a cheap method and abundant raw material was utilized to produce active carbon (SDAC). Physiochemical activation was utilized where potassium hydroxide   used as a chemical activating agent and carbon dioxide was used as a physical activating agent. Taguchi method of experimental design was used to find the optimum conditions of SDAC production. The produced SDAC was characterized using SEM to investigate surface morphology and BET to estimate the specific surface area. SDAC was used in aqueous lead ions adsorption. Adsorption process was modeled statistically and represented by an empirical model. The highest specific surface area of SDAC was 688.3 m2/gm. Langmuir and Freundlich isotherms were used to fit the adsorption process, where equilibrium data was best represented by Langmuir isotherm model. Pseudo-first order and pseudo-second order equations were used to study adsorption kinetics, lead adsorption on SDAC fitted pseudo- second order more adequately. Best removal efficiency was found to be 99.63% with highest adsorption capacity of 19.92 mg/g.

Keywords: Adsorption, activated carbon, sawdust, lead, physiochemical activation.

1. Introduction

Due to the wide range and the exaggerated uses of organic solvents, oxidizing agents, phenols and heavy metals in industry, they were accumulated in the environment which caused ecosystems deterioration.

Heavy metals category is one of the most lethal pollutants of surface and ground waters. Industrial effluents are the major source. Since most of heavy metals could not be degraded into benign components, removing the heavy metals before discharging waste waters into rivers   becomes necessary. Otherwise they could be harmful to the health and/or reduce drinking water quality [1].

According to the World Health Organization (WHO, 1984) and International Program of Chemical Safety (IPCS, 1988), the most poisonous metals are aluminum, zinc, mercury, arsenic, chromium, nickel, copper, cadmium and lead. The drinking water guideline value recommended by World Health Organization (WHO) and Iraqi standard regulation is 0.01 and 0.015 mg Pb/L.

Lead is found in freshwaters due to its wide uses in petroleum refining, batteries industry, preparation of nuclear fuels and electroplating. Lead causes severe damage to human organs e.g. kidneys, the brain, reproductive system, the liver and the nervous system [2].

As a result of the toxicity of the lead and its compounds, removal method has become an

important priority. There are various available means to reduce heavy metals levels from water including ion exchange, membrane filtration, chemical precipitation and reverse osmosis, but these methods generally require high cost and produce more lethal by products [3].

Adsorption on solid materials is one of the best existing methods for improving the water quality and the regulation of atmospheric and aquatic pollution, with active carbon being the most used adsorbent in industry. In the last years, worldwide consumption of active carbon has increased by an annual average of 5.5% , and it is anticipated to continue to do so at a higher rate in next years (8.1% in 2018)[4]. Thus, locally produced wastes such as saw dust, cow bones, and others were examined for preparing active carbon. Because of the low cost of those wastes, high percentage of carbonaceous contents and their abundancy, they were found to be of high potency in heavy metals adsorption.

The aim of this study is to optimize the production of activated carbon from sawdust by physiochemical activation method and to evaluate its adsorption potential for the lead ions aqueous solution. Adsorption isotherm fitting and kinetics studies were conducted to understand the behavior of lead ions onto SDAC. Effective parameters such as initial pH of the metal solutions, contact time, initial metal concentrations and temperature were investigated.

2. Materials and Methods
2.1. Adsorbate

Technical grade Lead nitrate ($Pb(NO_3)_2$) of 99.8% purity provided by Himedia- India was used to prepare stock solution of the Lead. Distilled water was used to prepare all solutions. A stock of 1000 mg/L was prepared by adding (1.68) gm of $Pb(NO_3)_2$ to a liter of distilled water. Other solutions were prepared by diluting the stock solution to the required concentrations. NaOH and HNO_3 solutions each of 0.1 M concentration were used to adjust pH value.

2.2. Preparation and Characterization of Activated Carbon

Saw Dust (SD) was obtained from local furniture workshops, Baghdad, Iraq as waste. The preparation methodology of SDAC is concisely illustrated in figure.1. The surface area was analyzed using Brunaure- Emmett-Teller (BET: HORIBA, SA-900 series, USA) through nitrogen adsorption isotherm at 77 K. In order to determine the shape of SDAC surface and pore characteristics, the samples were scanned using Scanning Electron Microscope (TESCAN, Vega III, Czech Republic).

2.3. Design of Experiments

Experimental design usually used to efficiently map the set of experiments to be conducted and to serve the following: understand the effect of the factors and/or model the relationship between response and factors with a minimum number of experiments [5]. Taguchi method was used in the optimization of SDAC production and in modelling of adsorption process due to its efficiency compared to other methodologies and its robustness. STATISTICA 10 (Stat Soft, Inc. USA) was used to design the set of experiments. Where L9 orthogonal array was chosen (2 factors, 3 levels) in SDAC preparation, and L25 array (4 factors, 4 levels) for adsorption process modelling.
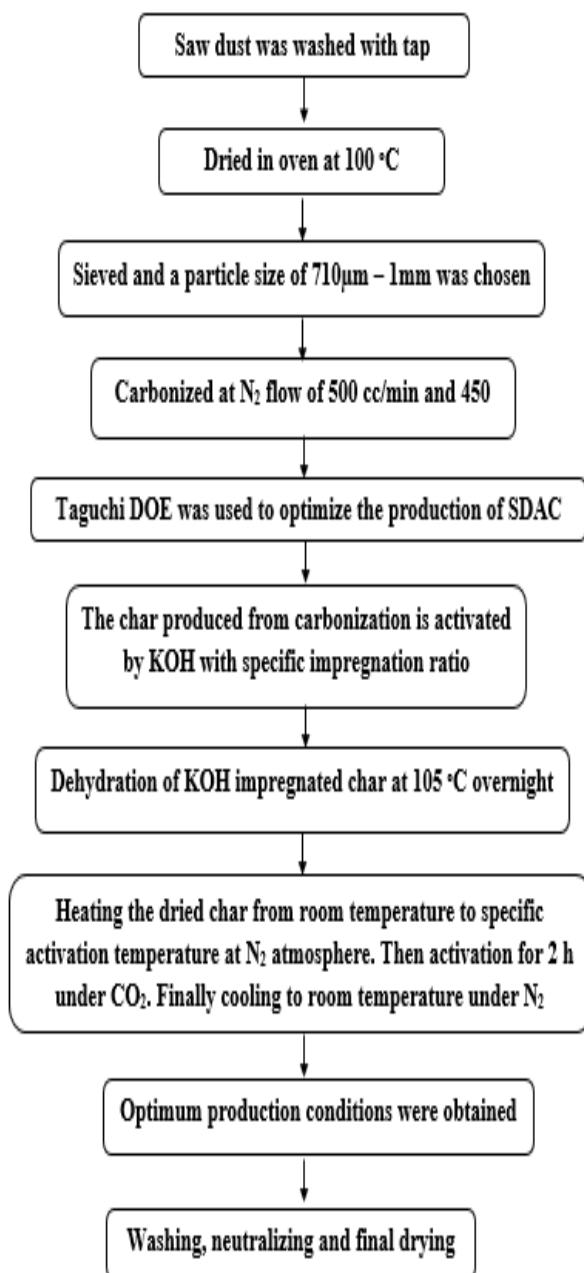
Fig. 1. Schematic diagram for the SDAC preparation steps.

2.4. Batch Equilibrium Studies

Bach mode adsorption experiments were conducted by adding specific amount of adsorbent to a 100 ml lead solution contained in 125 ml capped plastic containers. The containers were placed in an isothermal shaker (JSSI-300CL, JSR, Korea) at agitation speed of 180 rpm. After adsorption time was completed, all samples were filtered from the adsorbent with Whatmen filter paper to make it carbon free. The remaining concentration of the lead in each sample after adsorption was determined by atomic-absorption spectroscopy (Shimadzu AA6200, Japan). The lead adsorption capacity on SDAC was predicted according to:

$$q_e = \frac{(C_o - C_e)V}{W} \qquad \ldots (1)$$

where C_o and C_e are the concentrations of the Lead at initial and equilibrium conditions (mg/L) respectively; V is the volume (L); and W is the weight (g) of SDAC.

2.5. Adsorption Isotherm

Langmuir and Freundlich isotherm models were used to fit the equilibrium data. The linear form of the Langmuir [6] model is:

$$\frac{1}{q_e} = \frac{1}{q_m} + \frac{1}{(k_a q_m)} \frac{1}{C_e} \qquad \ldots (2)$$

where C_e (mg/L) is the concentration of the lead at equilibrium; q_e (mg/g) is the equilibrium adsorption capacity; q_m is the adsorption capacity for a complete monolayer (mg/g); K_a (L/mg) is the constant of adsorption equilibrium. The linear form of Freundlich [7] isotherm is:

$$\ln q_e = \ln K_F + \left(\frac{1}{n}\right) \ln C_e \qquad \ldots (3)$$

The constants K_F (mg/g) and n are Freundlich constants.

2.6. Kinetic Studies

The adsorption rate constants were predicted from the pseudo first-order and pseudo second-order kinetic equations. Pseudo first-order [8] expression is :

$$\log(q_e - q_t) = \log q_e - \frac{k_1 t}{2.303} \qquad \ldots (4)$$

where q_e and q_t (mg/g) are the adsorption capacities at equilibrium and at time t (min), respectively and k_1 (1/min) is the adsorption constant. The linear form of the pseudo second-order kinetic model [9] can give by:

$$\frac{t}{q_t} = \frac{1}{k_2 q_e^2} + \frac{1}{q_e} t \qquad \ldots (5)$$

where (q_e) is the adsorption capacity of equilibrium and the constant of second order k_2 (g/mg h) can be determined experimentally from the intercept and slope of t/qt versus t plot.

62

3. Results and Discussion
3.1. SDAC Production and Optimization

The experiments that were conducted are shown in table 1.

Table 1,
Preparation of SDAC experimental design array and the results for SSA and yield.

Runs	SDAC preparation variables		SDAC preparation responses	
	IR	Activation Temperature (C°)	Specific surface area (m2/gm)	Yield (%)
1	1:2	600	161.7	81.6
2	1:2	700	428.5	73.7
3	1:2	800	365.8	42
4	1:3	600	267.8	80.2
5	1:3	700	688.3	71.5
6	1:3	800	653	37.9
7	1:4	600	367.1	72.6
8	1:4	700	626.1	62.7
9	1:4	800	611.9	35.4

In SDAC preparation, the SSA increases as IR rises from 1:2 to 1:3. The clarification of this results is that the reduction of KOH occurs during activation process was transformed to potassium oxide by dehydration reaction. Potassium oxide reacts with carbon dioxide that is provided during physical activation to form K_2CO_3 which aids to form new pores and widen pores that formed during chemical activation. So it was recognized that above 420 C° (melting point of KOH), the surface area of carbon activated by KOH is more than the area of carbon activated by K_2CO_3 [10]. But when the IR reached to 1:4 the SSA decreased. This was probably due to excessive potassium hydroxide molecules decomposing into metal. As a result, metal deposition on the already developed pores might occur and lead to reduction of the surface area [11].

Regarding the activation temperature effect, it was perceived that as the temperature rises from 600 °C to 700 °C SSA increases. These results can be explained by the following: as the temperature increases, more KOH evaporates which enhances the surface porosity [12]. On the other hand, SSA decreased as the temperature reached to 800 °C, this is due to the fact that elevated activation temperatures cause pore dilation which lead to explosion/collapse of pores, that led to the lower values of specific surface area [13].

In general, the SDAC yield was found to be inversely proportional to both temperatures of activation and IR. As the temperature elevates more volatile components will be released due to intensified dehydration and elimination reaction that increase C-KOH and C-CO2 reaction rate which causes lower weights of SDAC [14]. Moreover, the yield decreased with increasing IR. Potassium hydroxide promotes the oxidation process, with high KOH ratio, the gasification of surface carbon atoms is the predominant reaction leading to increase in the weight loss of carbon [15].

3.2. SEM and BET Analysis

Fig. 2 shows the SEM images of SD and SDAC. It can be noticed that SDAC surface has developed pores in which there is a good probability for the lead to be adsorbed. BET surface area was 688.62m^2/g. Average pore diameter for SDAC was 5.675μm where it is larger than 50 nm that agrees with IUPAC categories of macro porous materials within the stated range [16]. The high SSA of the SDAC was a result of the used technique of activation. The activation process involved chemical and physical activating agents which are KOH and CO_2 respectively. However, the developed pores during carbonization enhanced the surface area by diffusing more CO_2 and KOH molecules inside the pores, therefore; the reaction between KOH-carbon and CO_2-carbon promoted leading to more pores in the activated carbon.
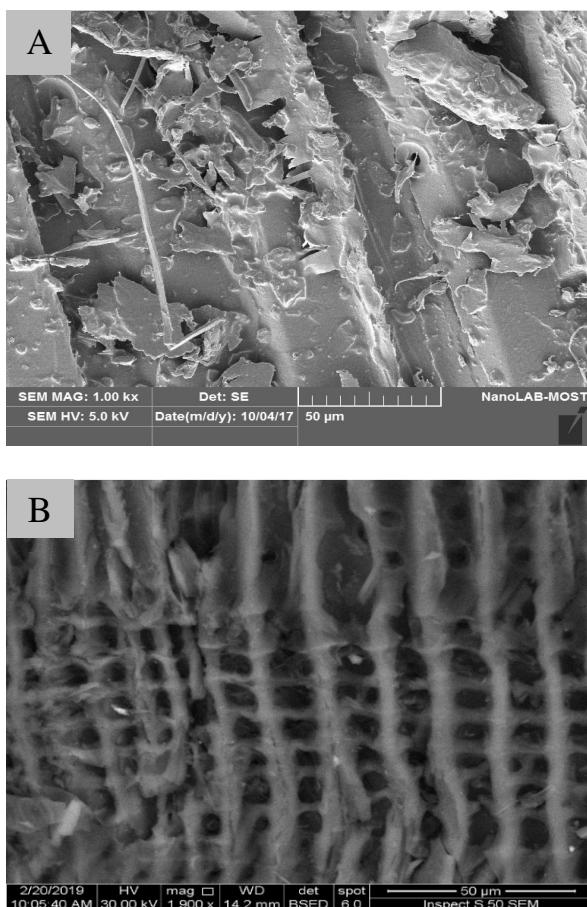
Fig. 2. SEM images (A) precursor and (B) SDAC (magnifications: 1000X)

3.3. Batch Equilibrium Studies

Batch adsorption experiments were conducted by adding 0.25 g of SDAC with 100 ml of prepared lead solution of various concentration (10, 20, 30, 50mg/l) with different initial solution pH ranging from 2 to 5. The experiments were accomplished in different contact times within the range of 10-40 minutes. The temperature range was 20-50 °C where the temperature was controlled by using thermal shaker.

Another set of experiments with time ranging from 30-300 minutes was conducted. Results showed that almost all of the experiments that have contact time larger than 30 minutes with no lead was remained, time range was change to 10-40 minutes.

3.4. Experimental Design and Empirical Model

The set of experiments that was designed by Taguchi method and their results are shown in Table 2.

Table 2,
Batch adsorption experiments and their response.

initial concentration (mg/L)	time (min)	Temperature (°C)	pH	equilibrium concentration (mg/L)
10	10	20	2	10
10	20	30	3	2.992
10	30	40	4	1.911
10	40	50	5	2.132
20	10	30	4	3.175
20	20	20	5	2.402
20	30	50	2	13.322
20	40	40	3	3.131
30	10	40	5	2.707
30	20	50	4	3.539
30	30	20	3	7.356
30	40	30	2	4.141
50	10	50	3	3.701
50	20	40	2	3.304
50	30	30	5	3.5
50	40	20	4	3.202

The obtained model with its four factors and their interaction is represented by:

$$Y = b_o + b_1X_1 + b_2X_2 + b_3X_3 + b_4X_4 + b_{12}X_1X_2 + b_{13}X_1X_3 + b_{14}X_1X_4 + b_{23}X_2X_3 + b_{24}X_2X_4 + b_{34}X_3X_4 + b_{11}X_1^2 + b_{22}X_2^2 + b_{33}X_3^2 + b_{44}X_4^2 \quad\quad \dots(6)$$

where b_0, b_1, b_2, b_3 and b_4 are the linear coefficients, b_{12}, b_{13}, b_{14}, b_{23}, b_{24} and b_{34} are the second-order interaction terms, and b_{11}, b_{22}, b_{33} and b_{44} are the quadratic terms of each factor. Y, X_1, X_2, X_3 and X_4 are the coded terms of equilibrium concentration, initial Lead concentration, time, temperature and pH, respectively.

The estimated values of the model coefficient, standard error of each model term, and its p value are shown in Table 3.

Table 4,
Model coefficients, standard error and terms p-values

	Estimate	Standard error	p- value
b0	0	-	-
b1	1.928	0.257	0.00
b2	-1.033	0.203	0.000002
b3	3.079	0.352	0.00
b4	-24.723	2.942	0.00
b12	0	-	-
b13	0	-	-
b14	0.031	0.002	0.05004
b23	0.004	0.00	0.00
b24	0.049	0.00	0.00
b34	0.037	0.003	0.00001
b11	0.004	0.001	0.00
b22	0	-	-
b33	-0.022	0.005	0.00
b44	1.603	0.466	0.001

b_o, b_{12}, b_{13} and b_{22} were eliminated from the model due to their insignificant values compared to others. Their elimination did not affect the accuracy of the predicted model.

3.5 Effects of Factors
3.5.1 Effect of Contact Time and Pb(II) Initial Concentration

The influence of adsorption time on the lead ions adsorbed by SDAC was investigated and presented in Fig. 2. It was observed that removing the lead ions was fast through the first 20 min and removing

efficiency of SDAC increased with the initial lead ion concentration. The adsorption was fast at the initial stage because of the high driving force which induced the metal ions to transfer rapidly from the bulk solution to the surface of SDAC [17]. With further increasing time, the availability of the uncovered surface area and the remaining active sites diminish and the decrease in the driving force makes it take long time to reach equilibrium for metal ions, and slowly diffusing into the intra-particle pores of the adsorbent. Thus, the adsorption rate becomes slower [18].

It is also clear from Fig. 2 that adsorption efficiency improved as the initial concentration of Pb (II) increased. This can be due to the fact that higher adsorbate concentration acts as a driving force for higher adsorption efficiency onto SDAC [13]. Similar trend of heavy metal adsorption, as a function of initial concentration, has also been reported previously by Igberase [19] and Trang [20].
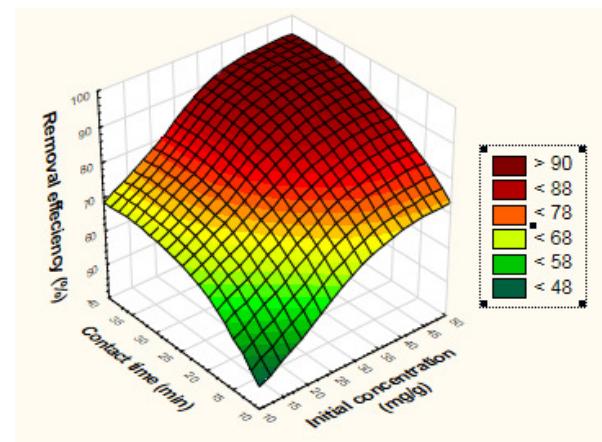
Fig. 2. Effect of contact time and initial concentration on removal efficiency.

3.5.2. Effect of pH and Temperature

The initial solution pH is the most significant factor to investigate the adsorption characteristic of an adsorbent because it affects not only surface charge of the adsorbent, but also the ionization degree and adsorbate speciation [21]. The effect of initial solution pH on the lead ion removal by SDAC is presented in Fig. 3. As the negative charge density on SDAC surface increases due to COOH ionization, the adsorbed lead will rise rapidly [22].

At pH = 5, the efficiency on adsorption reached its maximum value. In order to assure a true investigation of adsorption characteristics of SDAC and to avoid precipitation of the lead ions, all the experiments were run at pH <=5.0. This result is in line with Al-malack and Basaleh [23] and Shi [24].

As temperature rises, the solution viscosity will slightly decrease which enhances the diffusion rate of the lead into the pores of SDAC [25]. In addition to that, the high temperatures will break internal bonds at the edges of the active sites [26] which aids the enhancement of adsorption efficiency of the SDAC. Fig. 3 illustrates the direct proportion between temperature and efficiency of adsorption. As it can be seen from fig.3 that lead adsorption on SDAC is endothermic process. This result corresponds with Sulaymon [27] and Adebisi [3].
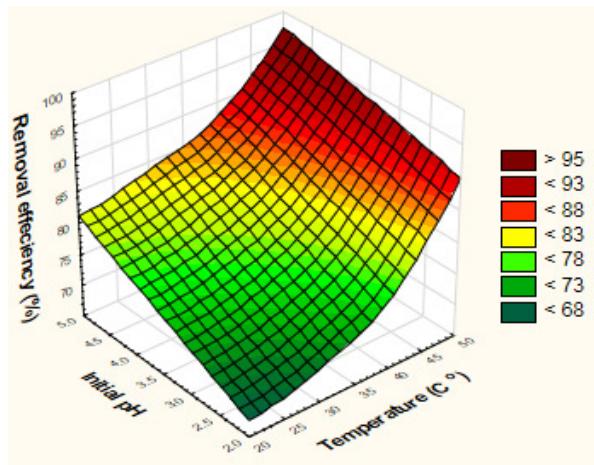
Fig. 3. Effect of initial pH and temperature on adsorption efficiency.

3.6 Adsorption Isotherm Studies

The adsorption data of Pb(II) on SDAC fitted Langmuir isotherm more adequately with R^2 value of 0.996. Fig.4 shows the plot of $1/C_e$ versus $1/q_e$. The results confirmed that the lead had formed a monolayer on the SDAC outer surface with monolayer full coverage adsorption capacity of 13.65 mg/g. Other studies had also confirmed the same results [28] and [29].
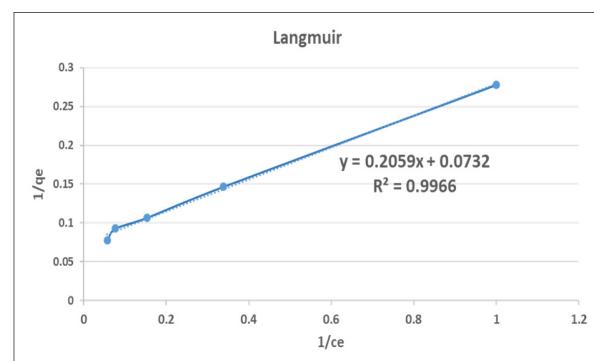
Fig. 4 Adsorption data fitted into Langmuir isotherm.

3.7. Kinetics Studies

To figure out the mechanism that controls the adsorption of the lead on SDAC, such as physical interactions and chemical reaction, pseudo-first-order and pseudo-second-order equations were utilized to model the kinetics of adsorption.

Fits better the experimental data (R^2 = 0.996) than the pseudo-first-order model (R^2 =0.974). The equilibrium adsorption capacity obtained from pseudo- second order (q_e) was 24.19 mg/g and second order constant k_2 = 0.0053 (g/mg h). Other researches had confirmed the same results [30] and [29].

4. Conclusion

The results of this study showed the active carbon that prepared from sawdust using physiochemical activation is a favorable adsorbent for the lead adsorption from aqueous solution over a wide range of conditions. Langmuir and Freundlich isotherm models were utilized to fit the data of equilibrium and the equilibrium data for SDAC were found to be well represented by the Langmuir isotherm. The kinetics of adsorption followed the pseudo second- order kinetic model. The empirical model represented the adsorption process accurately with R^2 value of 0.988. Based on the high range of removal efficiencies, SDAC can be used as a cost effective, and inexpensive substitute to the commercial activated carbons.

5. References

[1] Q. Dai, L. Ma, N. Ren, P. Ning, and Z. G. Longgui, "Research on the variations of organics and heavy metals in municipal sludge with additive acetic acid and modified phosphogypsum," *Water Res.*, vol. 155, no. 15 May 2015, pp. 42–55, 2019.

[2] A. Choinska-Pulit, J. Sobolczyk-bednarek, and L. Wojciech, "Optimization of copper , lead and cadmium biosorption onto newly isolated bacterium using a Box-Behnken design," Ecotoxicol. Environ. Saf., vol. 149, pp. 275–283, 2018.

[3] G. A. Adebisi and P. A. Alaba, "Equilibrium, Kinetic, and Thermodynamic Studies of Lead ion and Zinc ion Adsorption from Aqueous Solution onto Activated Carbon Prepared From Palm Oil Mill Effluent," J. Clean. Prod., vol. 148, pp. 958–968, 2017.

[4] J. Pallarés, A. González-Cencerrado, and I. Arauzo, "Production and characterization of activated carbon from barley straw by physical activation with carbon dioxide and steam," Biomass and Bioenergy, vol. 115, no. January, pp. 64–73, 2018.

[5] L. Massart and B. Vandeginste, Chemometrics and qualimetrics in chemical engineering. Newyork, NY: Princeton press, 1991.

[6] I. Langmuir, "The constitution and fundamental properties of solids and liquids.," J. Am. Chem. Soc., vol. 182, pp. 2221–2295, 1916.

[7] H. Freundlich, "Capillary anf colloid chemistry. By Prof. H. Freundlich. Translated by H. Stafford Hatfield.," J. Phys. Chem, vol. 57, pp. 385–470, 1925.

[8] Y.-S. Ho, "Citation review of Lagergren kinetic rate equation on adsorption reactions," Scientometrics, vol. 59, no. 1, pp. 171–177, 2004.

[9] H. P. Boehm, "Some aspects of the surface chemistry of carbon blacks and other carbons," Carbon N. Y., vol. 32, no. 5, pp. 759–769, 1994.

[10] S. Mopoung, P. Moonsri, W. Palas, and S. Khumpai, "Characterization and Properties of Activated Carbon Prepared from Tamarind Seeds by KOH Activation for Fe (III) Adsorption from Aqueous Solution," Sci. World J., vol. 2015, pp. 150–159, 2015.

[11] A. Borhan, M. F. Taha, and A. A. Hamzah, "Characterization of Activated Carbon from Wood Sawdust Prepared via Chemical Activation using Potassium Hydroxide," Adv. Mater. Res., vol. 832, pp. 132–137, 2014.

[12] T. C. Chandra, M. M. Mirna, Y. Sudaryanto, and S. Ismadji, "Adsorption of basic dye onto activated carbon prepared from durian shell: Studies of adsorption equilibrium and kinetics," Chem. Eng. J., vol. 127, no. 1–3, pp. 121–129, 2007.

[13] A. Nayak, B. Bhushan, V. Gupta, and P. Sharma, "Chemically activated carbon from lignocellulosic wastes for heavy metal waste-water remediation: effect of activation conditions.," J. Colloid Interface Sci., vol. 493, pp. 228–240, 2017.

[14] M. Danish, R. Hashim, M. N. M. Ibrahim, and O. Sulaiman, "Optimized preparation for large surface area activated carbon from date (Phoenix dactylifera L.) stone biomass," Biomass and Bioenergy, vol. 61, no. 320, pp. 167–178, 2014.

[15] Y. Sudaryanto, S. B. Hartono, W. Irawaty, H. Hindarso, and S. Ismadji, "High surface area activated carbon prepared from cassava peel by chemical activation," Bioresour. Technol., vol. 97, no. March 2005, pp. 734–739, 2006.

[16] S. Norouzi et al., "Preparation, characterization and Cr(VI) adsorption evaluation of NaOH-activated carbon produced from Date Press Cake; an agro-industrial waste," Bioresour. Technol., vol. 258, no. Vi, pp. 48–56, 2018.

[17] A. H. M. G. Hyder, S. A. Begum, and N. O. Egiebor, "Adsorption isotherm and kinetic studies of hexavalent chromium removal from aqueous solution onto bone char," J. Environ. Chem. Eng., vol. 3, no. 2, pp. 1329–1336, 2014.

[18] I. Ullah, R. Nadeem, M. Iqbal, and Q. Manzoor, "Biosorption of chromium onto native and immobilized sugarcane bagasse waste biomass," Ecol. Eng., vol. 60, pp. 99–107, 2013.

[19] E. Igberase, A. Ofomaja, and P. O. Osifo, "Enhanced heavy metal ions adsorption by 4'aminobenzoic acid grafted on chitosan/epichlorohydrin composite: Kinetics, isotherms, thermodynamics and desorption studies," Int. J. Biol. Macromol., vol. 123, pp. 664–676, 2018.

[20] M. Trang, T. Duc, V. Tu, and M. Khai, "Removal and recovery of lead from wastewater using an integrated system of adsorption and crystallization," J. Clean. Prod.,

vol. 213, pp. 1204–1216, 2019.

[21] M. Imamoglu and O. Tekir, "Removal of copper (II) and lead (II) ions from aqueous solutions by adsorption on activated carbon from a new precursor hazelnut husks," Desalination, vol. 228, pp. 108–113, 2008.

[22] P. Miretzky, C. Munoz, and A. Carrillo-chavez, "Experimental binding of lead to a low cost on biosorbent: Nopal (Opuntia streptacantha)," Bioresour. Technol., vol. 99, pp. 1211–1217, 2008.

[23] M. H. Al-malack and A. A. Basaleh, "Adsorption of heavy metals using activated carbon produced from municipal organic solid waste organic solid waste," Desalin. Water Treat., vol. 57, no. 51, pp. 24519–24531, 2016.

[24] Q. Shi, A. Terracciano, Y. Zhao, C. Wei, C. Christodoulatos, and X. Meng, "Evaluation of metal oxides and activated carbon for lead removal : Kinetics , isotherms , column tests , and the role of co-existing ions," Sci. Total Environ., vol. 648, pp. 176–183, 2019.

[25] S. Chen, J. Zhang, C. Zhang, Q. Yue, Y. Li, and C. Li, "Equilibrium and kinetic studies of methyl orange and methyl violet adsorption on activated carbon derived from Phragmites australis," Desalination, vol. 252, no. 1–3, pp. 149–156, 2010.

[26] J. Acharya, J. Sahu, C. Mohanty, and B. Meikap, "Removal of lead (II) from wastewater by activated carbon developed from Tamarind wood by zinc chloride activation," Chem. Eng. J. J., vol. 149, pp. 249–262, 2009.

[27] A. H. Sulaymon, A. A. Mohammed, and T. J. Al-musawi, "Competitive biosorption of lead , cadmium , copper , and arsenic ions using algae," Environ. Sci. Pollut. Res., vol. 20, no. 5, pp. 3011–3023, 2013.

[28] K. G. Sreejalekshmi, K. A. Krishnan, and T. S. Anirudhan, "Adsorption of Pb (II) and Pb (II) -citric acid on sawdust activated carbon : Kinetic and equilibrium isotherm studies," J. Hazard. Mater. J., vol. 161, pp. 1506–1513, 2009.

[29] F. Cao, C. Lian, J. Yu, H. Yang, and S. Lin, "Study on the adsorption performance and competitive mechanism for heavy metal contaminants removal using novel multi-pore activated carbons derived from recyclable long-root Eichhornia crassipes," Bioresour. Technol., vol. 267, pp. 211–218, 2019.

[30] M. Ghasemi, M. Naushad, N. Ghasemi, and Y. Khosravi-fard, "A novel agricultural waste based adsorbent for the removal of Pb (II) from aqueous solution : Kinetics , equilibrium and thermodynamic studies," J. Ind. Eng. Chem., vol. 20, no. 2, pp. 454–461, 2014.

أمتزاز المعادن الثقيلة من محلول مائي على كاربون منشط منتج من نشارة الخشب

مرح وليد خالد*   **سامي داود سلمان****

*،**قسم الهندسة الكيميائية الاحيائية/ كلية الهندسة الخوارزمي/ جامعة بغداد

**البريد الالكتروني:sami.albayati@gmail.com

الخلاصة

نتيجة للاستعمالات الواسعة للرصاص في الصناعة، بالإضافة الى أن اثاره الخطرة، وجب البحث عن طريقه فعاله واقتصاديه لإزالته من المياه العادمة. في هذه الدراسة، تم استخدام نشارة الخشب، كماده اوليه رخيصة، لإنتاج الكاربون المنشط. تم استخدام طريقه فيزيائية كيميائية للتفعيل، حيث تم استخدام هيدروكسيد البوتاسيوم كعامل تفعيل كيميائي وثنائي أوكسيد الكربون كعامل تفعيل فيزيائي. تم استخدام طريقة تاغوشي لتصميم التجارب لإيجاد أفضل الظروف لتحضير الكاربون المنشط من نشارة الخشب. تم تشخيص الكاربون المنتج بالمجهر الالكتروني للتحقق من شكله السطحي وتم استخدام ال(BET) لمعرفة مساحته السطحية. تم استخدام الكاربون المنتج من نشارة الخشب لامتزاز ايونات الرصاص من المحاليل المائية. تم تمثيل عملية الامتزاز رياضيا بواسطة معادله قياسيه تجريبية. اعلى مساحة سطحيه تم الحصول عليها هي ٦٨٨,٣ م٢/غم. تم استخدام معادلة لانغماير وفرينداليتش لتمثيل عملية الامتزاز ، حيث كانت العملية متطابقة بصورة كبيرة مع نموذج لانغماير. تم استخدام معادلة الدرجة الأولى والدرجة الثانية الخاصة بدرجة حركيه الامتزاز، حيث كانت عملية الامتزاز متوافقة بصورة كبيرة مع معادلة الدرجة الثانية. أعلى كفاءه امتزاز تم الحصول عليها بلغت ٩٩,٦٣% مع أعلى قدرة امتزاز تصل الى ١٩,٩٢ ملغم/غم.